LETTERS
PUBLISHED ONLINE: 30 JANUARY 2011 | DOI: 10.1038/NPHOTON.2010.312
nature photonics

A planar dielectric antenna for directional single-photon emission and near-unity collection efficiency

K. G. Lee†, X. W. Chen†, H. Eghlidi, P. Kukura, R. Lettow, A. Renn, V. Sandoghdar and S. Götzinger*

Single emitters have been considered as sources of single photons in various contexts, including cryptography, quantum computation, spectroscopy and metrology[1–3]. The success of these applications will crucially rely on the efficient directional emission of photons into well-defined modes. To accomplish high efficiency, researchers have investigated microcavities at cryogenic temperatures[4,5], photonic nanowires[6,7] and near-field coupling to metallic nano-antennas[8–10]. However, despite impressive progress, the existing realizations substantially fall short of unity collection efficiency. Here, we report on a theoretical and experimental study of a dielectric planar antenna, which uses a layered structure to tailor the angular emission of a single oriented molecule. We demonstrate a collection efficiency of 96% using a microscope objective at room temperature and obtain record detection rates of ∼50 MHz. Our scheme is wavelength-insensitive and can be readily extended to other solid-state emitters such as colour centres[11,12] and semiconductor quantum dots[13,14].

One of the most powerful and versatile approaches to the generation of single photons takes advantage of the property whereby a single quantum-mechanical two-level system cannot emit two photons simultaneously, as each excitation and emission cycle requires a finite time. Unfortunately, such single-photon sources are intrinsically inefficient, because their radiation spreads over a 4π solid angle and cannot be fully captured by conventional optics. Several years ago, a simple avenue for efficient photon collection was proposed by Koyama and colleagues in the context of fluorescence microscopy[15], where emitters were placed at the interface between two media with large refractive index contrast[15–17]. Such a structure can be viewed as a dielectric antenna[18] in which the dipolar radiation of the emitter is funnelled into the high-index substrate. The black trace in Fig. 1a shows the angular emission of a dipole sitting close to an interface and oriented perpendicular to it. Despite the strongly modified radiation pattern, one finds that 14% of the light is still lost to the upper half-space, and, more importantly, a considerable amount of light is directed to very large angles in the lower substrate, which are not accessible to the collection optics. Luan and colleagues observed modifications of the emission pattern when molecules were randomly embedded in a dielectric film at the interface, but did not discuss a deterministic design for optimizing the collection efficiency into well-defined modes[19]. In this Letter, we address these issues by carefully embedding an oriented emitter in a dielectric layer that is engineered on top of the high-index substrate and obtain unprecedented photon collection efficiencies, directionality and count rates.

To provide an intuitive explanation of our antenna design, let us decompose the radiation of a dipolar emitter into plane waves and consider the propagation of each component[20,21]. This strategy will also be the basis of the calculations that follow in this work. We start by considering a structure that consists of a lower output substrate with refractive index n_1 in contact with an upper medium that contains the emitter and has an index $n_2 < n_1$. To avoid feeding output modes at large angles, we set the distance h between the emitter and the interface to be larger than a characteristic evanescent length[15,16]. This means that the radiation of the emitter into the lower half-space couples only to angles $\theta_1 < \sin^{-1}(n_2/n_1)$ in the substrate, but one loses the part that is emitted parallel to the interface and upwards. To get around this problem, we limit the thickness of the upper layer and consider a third medium with refractive index $n_3 < n_2$, as shown in Fig. 1b. This construction channels the emission of the molecule into quasi-waveguide modes of the middle layer with horizontal wave numbers k_ρ in the range $k_0 n_3 < k_\rho < k_0 n_2$, where k_0 is the vacuum wavenumber. These modes then leak into the substrate at well-defined angles below $\sin^{-1}(n_2/n_1)$ and can be collected with a commercial microscope objective.

For the high-index substrate we chose a sapphire cover glass with $n_1 = 1.78$. A thin film of the polymer polyvinyl alcohol (PVA) with $n_2 = 1.50$ formed the quasi-waveguide, and the top layer was air ($n_3 = 1$). The red and green curves in Fig. 1a present two examples of outcoupled modes in the n_1 medium computed for two choices of PVA thickness t and emitter–interface distance h.

The corresponding colour-coded curves in the inset illustrate the same data in a polar representation. We find that in each case more than 95.5% of the emitted light falls in a cone with a half-angle of 68°, corresponding to a numerical aperture of 1.65. In addition, the contour plot in Fig. 1c shows that the outcoupling efficiency is quite insensitive to variations in t and h, making the performance of such a device highly tolerant to fabrication imperfections. This is in great contrast to an arrangement comprising a simple interface[15], where the collection efficiency drops rapidly with h. We emphasize that the normal orientation of the emitter is an integral part of our antenna design. It is also important to note that the modification of the spontaneous emission rate in our structure is negligible compared to an emitter in bulk PVA (see Supplementary Information). Furthermore, the broadband design of the antenna prevents a change of the fluorescence spectrum, even if it spreads over tens of nanometres (see Supplementary Information). These features ensure that the antenna does not perturb the intrinsic photophysical properties of the emitter.

As emitters we used single terrylene molecules with a fluorescence maximum at 580 nm. To achieve photostability at room temperature, we embedded terrylene in a thin (20 nm) crystalline *p*-terphenyl matrix[22]. This system also has the great advantage

Laboratory of Physical Chemistry and optETH, ETH Zürich, CH-8093 Zürich, Switzerland; †These authors contributed equally to this work.
*e-mail: stephan.goetzinger@phys.chem.ethz.ch

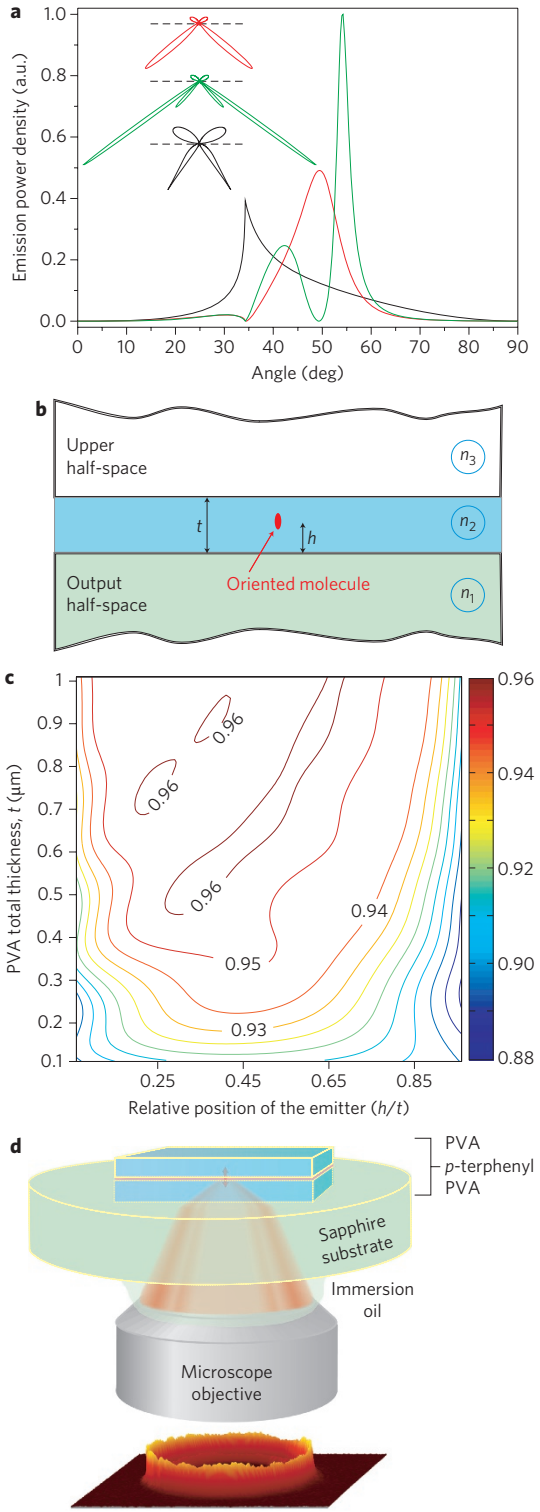

Figure 1 | Emission properties of a vertically oriented dipole close to a dielectric planar antenna. a, Emitted power density as a function of the collection angle. Black curve: dipole at a distance of 5 nm from the interface of two media with a refractive index ratio of 1.78 (air–sapphire). Red and green: dipoles in a structure as described in **b** with middle layer thickness, $t = 350$ nm and 600 nm, respectively; the emitter was placed at $h = 200$ nm in both cases. Insets: the same data in polar coordinates. The upper part of each figure is magnified by a factor of ten for better visibility. **b**, Sketch of the layered dielectric antenna. **c**, Contour plot of the fraction of emitted power that enters the lower substrate within a numerical aperture of 1.65 as a function of t and h. **d**, Schematics of the experimental arrangement.

that the terrylene molecules are oriented perpendicular to the plane of the p-terphenyl film. Our calculations show that an ultrathin film within the middle layer does not influence the theoretical predictions (Fig. 1a), so the emitters can be treated as dopants directly placed in the second medium, as suggested by Fig. 1b. The schematics of the final device are shown in Fig. 1d. We first report on studies of a sample made from two PVA layers sandwiching a p-terphenyl film on top of a sapphire cover glass with parameters $t = 350 \pm 20$ nm and $h = 200 \pm 20$ nm. Next we show results for the case of $t = 600 \pm 20$ nm. The sapphire substrate was index-matched on the other side by an immersion oil suitable for a microscope objective with a numerical aperture of 1.65 (Olympus Apo ×100). Details of sample fabrication as well as the excitation and detection of single-molecule fluorescence are provided in the Methods.

To quantify the collection efficiency of our antenna structure, we define the parameter $\eta = S_{co}/S_{em}$ as the ratio of the collected power that enters the microscope objective (S_{co}) to the total power emitted by a single molecule (S_{em}), both in units of photons per second. The latter is given by the product $N_2 k_{21}$, where N_2 is the population of the excited state (2) and k_{21} is the rate of its radiative decay to the ground state (1). As outlined in the energy level scheme in the inset of Fig. 2a, the triplet state (3) also affects the absorption and emission processes. The time trace in the inset of Fig. 2b displays an example of the resulting intermittent on- and off-times. A complete knowledge of all rates and populations requires thorough investigation[23]; however, as we show below, S_{em} can also be evaluated in a less tedious fashion.

The spontaneous emission rate k_{21} is given by the inverse of the rise time τ of the autocorrelation function $g^{(2)}$ in the weak excitation limit. At finite excitation powers, τ is reduced according to $\tau^{-1} = k_{12} + k_{21}$ where k_{12} is the intensity-dependent excitation rate. Figure 2a shows an example of a Hanbury–Brown and Twiss measurement. The red curve is a fit to the experimental data, taking into account the finite time resolution of the avalanche photodiodes and allowing a residual fluorescence background. Figure 2b plots the fluorescence signal as a function of the excitation power. By measuring $g^{(2)}$ and examining τ for a variety of excitation powers, we determined $k_{21} = 1.26 \times 10^8\ \mathrm{s}^{-1}$ and k_{12} for each experiment (see Supplementary Information). Note that the quantum efficiency of terrylene in p-terphenyl is near unity, so the measured excited-state decay rate is solely of a radiative nature[24].

Published studies[23] and work in our own laboratory reveal that k_{23}^{-1} and k_{31}^{-1} are orders of magnitude longer than τ (see also on–off-times in the inset of Fig. 2b). Consequently, the molecule can be considered as a two-level system during its on-time, allowing us to write $N_2^{on} = k_{12}/(k_{12} + k_{21})$ at steady state $(\mathrm{d}N_2/\mathrm{d}t = 0)$. Hence, the photon emission rate during the on-time can be obtained according to $S_{em}^{on} = N_2^{on} k_{21}$. Now, to compute the long-term total emission rate (S_{em}^{tot}), one has to account for the fraction of time the molecule is dark, arriving at $S_{em}^{tot} = N_2^{on} k_{21}(1 - \text{off-time})$. We determined the off-times at different excitation powers directly from recorded time traces (see Supplementary Information). At the highest excitation power of 7 mW in our experiment (Fig. 2b) we found the off-time to be 5% and $N_2^{on} = 0.82$, so that the emitted power amounted to $0.82 \times (1.26 \times 10^8\ \mathrm{s}^{-1}) \times (0.95) = 9.8 \times 10^7$ photons per second.

To deduce S_{co} from the detected count rate (S_{de}), we quantified the transmission loss of the optical path and the quantum efficiency of the charge coupled device (CCD) and found an overall detection efficiency of 51.8% for registering a count per collected photon. Furthermore, we assessed the background level at each excitation power by evaluating the CCD image away from the image spot of the terrylene molecule for each excitation power that was used in the correlation measurements. At the maximum excitation power of 7 mW, we found $S_{co} = 9.4 \times 10^7$. Finally, we determined the collection

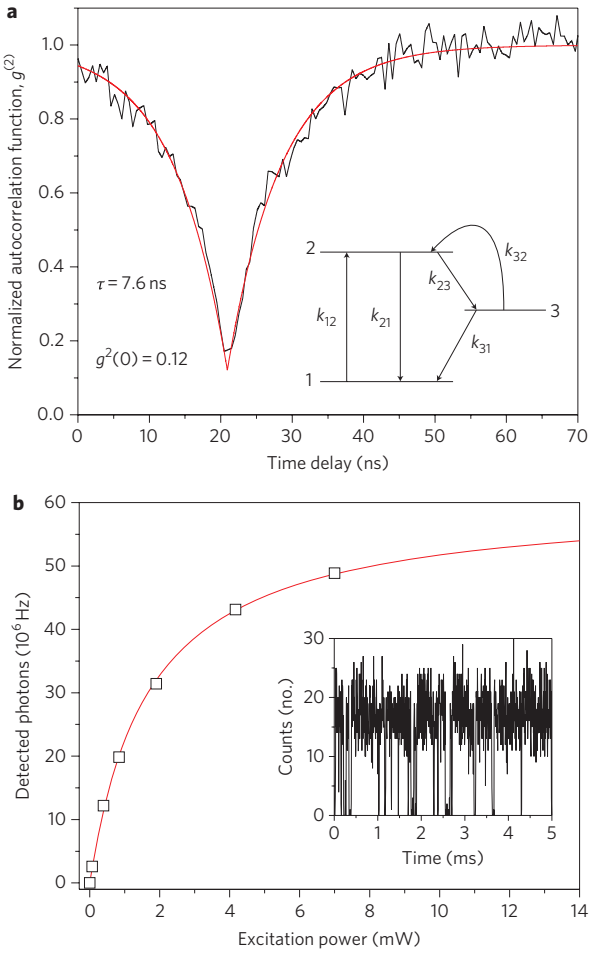

Figure 2 | Photophysics of the single-photon source. a, Second-order photon correlation measurement at an excitation power of 0.07 mW with an integration time of 20 s. At higher excitation power we could measure the second-order correlation function in less than 1 s. Inset: simplified level scheme. **b**, Fluorescence signal versus excitation power. The maximum photon detection rate is 4.9×10^7 Hz at the highest excitation power of 7 mW. The background has been subtracted from the data. Inset: a portion of a time-tagged time-resolved experiment with a time bin size of 5 μs.

efficiency for every excitation power and obtained $\eta = 96\% \pm 3\%$. This outcome is in excellent agreement with the theoretically expected value of 96% for a structure with $t = 350 \pm 20$ nm and $h = 200 \pm 20$ nm, sandwiching a *p*-terphenyl film of thickness 20 ± 5 nm. The error accounts for all uncertainties in the setup calibrations and fitting procedures (see Supplementary Information).

To examine the angular distribution of the emission pattern and its directionality, we imaged the intensity distribution at the back focal plane of the microscope objective. The inset of Fig. 3a plots the recorded image, and the blue curve in the main figure shows the normalized power distribution as a function of the collection angle (numerical aperture). The red trace in Fig. 3a confirms that the theoretical calculations agree remarkably well with the experimental data. The emission is mainly confined in one lobe centred around 51.5° with a full-width at half-maximum of 10°. The directivity of the emission, defined as the ratio of the maximum angular power density to the averaged power density in 4π solid angle[18], is found to be 11.8. The resulting beam is very close to a radially polarized doughnut mode, which has been recently discussed in various contexts[25]. It is also possible to convert the observed output modes to other modes such as the fundamental mode of an optical fibre with very high fidelity[26].

In Fig. 3b, we display the outcome of the same experiment performed for another structure with $t = 600$ nm and $h = 200$ nm. Again, the experiment (blue) reproduces the theoretical predictions (red) very well. Now the directivity of emission reaches 22.0, and the thicker PVA layer can now support an additional quasi-waveguide mode, giving rise to the second emission lobe.

Having established a record in collection efficiency, directional emission and high count rates from a single emitter, we stress the flexibility and potential of our antenna concept for use in solid-state systems. A major advantage is that, in contrast to plasmonic structures, which suffer from losses and a strong dependence on nanoscopic shape and size variations, our design strategy is insensitive to operation wavelength and fabrication imperfections. Thus, the scheme is readily applicable to semiconductor quantum dots, diamond colour centres, or solid-state ions alike, if their transition dipole moments are oriented normal to the antenna plane. Moreover, replacing oil-based microscope objectives with solid immersion lenses will allow a more compact device both for room-temperature and cryogenic usage. One of the exciting

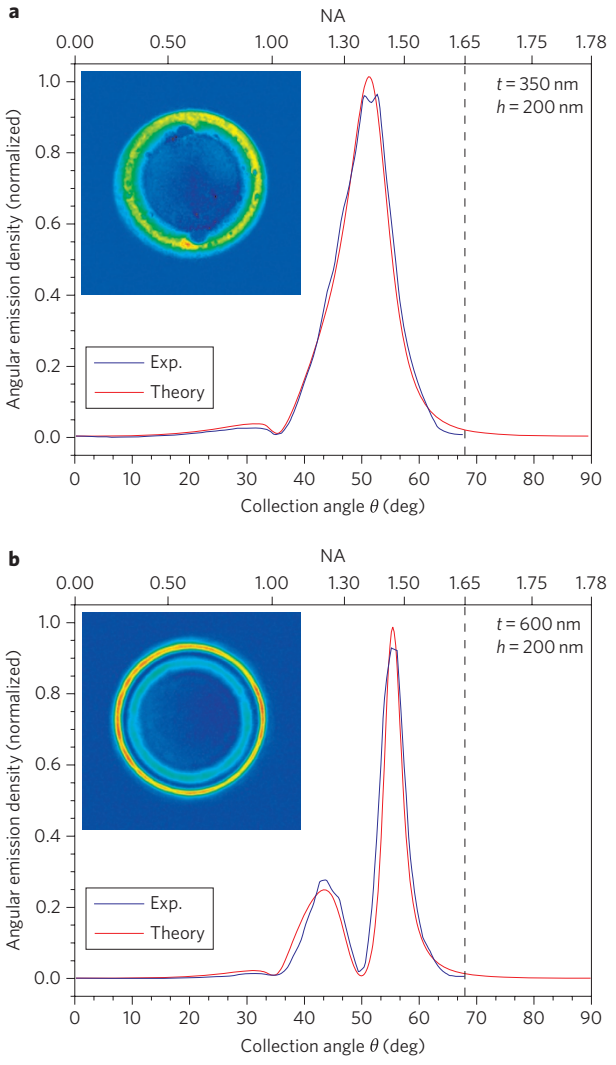

Figure 3 | Angular distribution of the emission. a, Theoretical and measured angular emission intensity for a structure with $t = 350$ nm and $h = 200$ nm. Inset: back focal plane image of the single molecule. **b**, As in **a** but for a structure with $t = 600$ nm and $h = 200$ nm. Theoretical curves in both figures account for an angular resolution of 2° imposed by the pixilation of the CCD camera. The vertical dashed line indicates the maximum collection angle of the objective.

prospects will be the realization of an ultrabright source of Fourier-limited photons[27], which play a central role in proposals in quantum information science[28]. In particular, we envision using such a single-photon source for excitation and spectroscopy of a molecule that is embedded in an identical second structure. The modification of the molecular dipolar pattern to a directional emission will allow mode matching between the illumination and the emitter, leading to highly efficient coupling[29]. Further potential for our bright non-classical light source lies in microscopy and spectroscopy beyond shot noise[1,30] and as a primary intensity standard for metrology[2,3].

Methods

Sample fabrication. Sapphire cover glasses were first cleaned in acetone and toluene to remove organic contamination. To fabricate well-defined organic films, PVA (Aldrich; $M_w = 89{,}000$–$98{,}000$) was dissolved in deionized water and 250 µl of the PVA/water solution was spin-coated (20 s with 2,000 rpm) onto a clean sapphire cover glass. By changing the PVA concentration we were able to control the film thickness. A PVA concentration of 0.04 g ml^{-1} resulted in a film thickness of 200 ± 20 nm, as determined by atomic force microscopy measurements. We protected this organic layer with 4 nm of Al_2O_3 using atomic layer deposition (Picosun Sunale R-150B). This film does not alter the properties of the sample and only serves to protect the PVA film against the solvent when the second PVA layer is spin-coated (see below). We then spin-coated a solution of toluene containing terrylene and p-terphenyl, following the procedure described in ref. 22. Finally, we spin-coated another PVA film using the same spin-coating parameters as above. Its thickness was again confirmed by atomic force microscopy measurements.

Experimental setup. To excite the terrylene molecules, we used a continuous-wave laser at a wavelength of 532 nm. This light was focused to an area of $\sim 2\ \mu m \times 1\ \mu m$ via total internal reflection through the microscope objective. By setting the incident light to be p-polarized, we ensured efficient excitation of the vertically oriented molecular dipole moments[22]. Photons emitted by the molecules were collected by the same microscope objective, separated from the excitation light with a long-pass filter (Semrock, 538 nm), and detected by a CCD (Andor iXon, 95% quantum efficiency at 605 nm) or a Hanbury–Brown and Twiss photon correlator.

Received 23 August 2010; accepted 6 December 2010; published online 30 January 2011

References

1. Lounis, B. & Orrit, M. Single-photon sources. *Rep. Prog. Phys.* **68,** 1129–1179 (2005).
2. Scheel, S. Single-photon sources—an introduction. *J. Mod. Opt.* **56,** 141–160 (2009).
3. Polyakov, S. V. & Migdall, A. L. Quantum radiometry. *J. Mod. Opt.* **56,** 1045–1052 (2009).
4. Pelton, M. *et al.* Efficient source of single photons: a single quantum dot in a micropost microcavity. *Phys. Rev. Lett.* **89,** 233602 (2002).
5. Strauf, S. *et al.* High-frequency single-photon source with polarization control. *Nature Photon.* **1,** 704–708 (2007).
6. Claudon, J. *et al.* A highly efficient single-photon source based on a quantum dot in a photonic nanowire. *Nature Photon.* **4,** 174–177 (2010).
7. Babinec, T. M. *et al.* A diamond nanowire single-photon source. *Nature Nanotech.* **5,** 195–199 (2010).
8. Chang, D. E., Sorensen, A. S., Hemmer, P. R. & Lukin, M. D. Strong coupling of single emitters to surface plasmons. *Phys. Rev. B.* **76,** 035420 (2007).
9. Chen, X. W., Sandoghdar, V. & Agio, M. Highly efficient interfacing of guided plasmons and photons in nanowires. *Nano Lett.* **9,** 3756–3761 (2009).
10. Curto, A. G. *et al.* Unidirectional emission of a quantum dot coupled to a nanoantenna. *Science* **329,** 930–933 (2010).
11. Kurtsiefer, C., Mayer, S., Zarda, P. & Weinfurter, H. Stable solid-state source of single photons. *Phys. Rev. Lett.* **85,** 290–293 (2000).
12. Simpson, D. A. *et al.* A highly efficient two level diamond based single photon source. *Appl. Phys. Lett.* **94,** 203107 (2009).
13. Michler, P. *et al.* Quantum correlation among photons from a single quantum dot at room temperature. *Nature* **406,** 968–970 (2000).
14. Ward, M. B. *et al.* On-demand single-photon source for 1.3 µm telecom fiber. *Appl. Phys. Lett.* **86,** 201111 (2005).
15. Koyama, K., Yoshita, M., Baba, M., Suemoto, T. & Akiyama, H. High collection efficiency in fluorescence microscopy with a solid immersion lens. *Appl. Phys. Lett.* **75,** 1667–1669 (1999).
16. Lukosz, W. & Kunz, R. E. Light emission by magnetic and electric dipoles close to a plane dielectric interface. II. Radiation patterns of perpendicular oriented dipoles. *J. Opt. Soc. Am.* **67,** 1615–1619 (1977).
17. Brokmann, X., Giacobino, E., Dahan, M. & Hermier, J. P. Highly efficient triggered emission of single photons by colloidal CdSe/ZnS nanocrystals. *Appl. Phys. Lett.* **85,** 712–714 (2004).
18. Balanis, C. A. *Antenna Theory* (Wiley-Interscience, 2005).
19. Luan, L. *et al.* Angular radiation pattern of electric dipoles embedded in a thin film in the vicinity of a dielectric half space. *Appl. Phys. Lett.* **89,** 031119 (2006).
20. Neyts, K. A. Simulation of light emission from thin-film microcavities. *J. Opt. Soc. Am. A* **15,** 962–971 (1998).
21. Chen, X., Choy, W. C. H. & He, S. Efficient and rigorous modeling of light emission in planar multilayer organic light-emitting diodes. *J. Disp. Technol.* **3,** 110–117 (2007).
22. Pfab, R. J. *et al.* Aligned terrylene molecules in a spin-coated ultrathin crystalline film of *p*-terphenyl. *Chem. Phys. Lett.* **387,** 490–495 (2004).
23. Fleury, L., Segura, J. M., Zumofen, G., Hecht, B. & Wild, U. P. Nonclassical photon statistics in single-molecule fluorescence at room temperature. *Phys. Rev. Lett.* **84,** 1148–1151 (2000).
24. Buchler, B. C., Kalkbrenner, T., Hettich, C. & Sandoghdar, V. Measuring the quantum efficiency of the optical emission of single radiating dipoles using a scanning mirror. *Phys. Rev. Lett.* **95,** 063003 (2005).
25. Dorn, R., Quabis, S. & Leuchs, G. Sharper focus for a radially polarized light beam. *Phys. Rev. Lett.* **91,** 233901 (2003).
26. Ramachandran, S., Kristensen, P. & Yan, M. F. Generation and propagation of radially polarized beams in optical fibers. *Opt. Lett.* **34,** 2525–2527 (2009).
27. Lettow, R. *et al.* Quantum interference of tunably indistinguishable photons from remote organic molecules. *Phys. Rev. Lett.* **104,** 123605 (2010).
28. Knill, E., Laflamme, R. & Milburn, G. J. A scheme for efficient quantum computation with linear optics. *Nature* **409,** 46–52 (2001).
29. Zumofen, G., Mojarad, N. M., Sandoghdar, V. & Agio, M. Perfect reflection of light by an oscillating dipole. *Phys. Rev. Lett.* **101,** 180404 (2008).
30. Celebrano, M. *et al.* Efficient coupling of single photons to single plasmons. *Opt. Express* **18,** 13829–13835 (2010).

Acknowledgements

The authors acknowledge financial support from the Swiss National Foundation (SNF) and ETH Zurich (QSIT). Thanks also go to M. Agio and G. Zumofen for helpful discussions and E. Ikonen for fruitful exchange regarding the potential of single-photon sources for metrology.

Author contributions

K.G.L. and H.E. performed the experiments reported here. P.K., R.L. and K.G.L. suggested and performed the first experiments. X.W.C. suggested the use of layered structures and performed the calculations. A.R., S.G. and V.S. supervised the project. S.G. and V.S. wrote the paper.

Additional information

The authors declare no competing financial interests. Supplementary information accompanies this paper at www.nature.com/naturephotonics. Reprints and permission information is available online at http://npg.nature.com/reprintsandpermissions/. Correspondence and requests for materials should be addressed to S.G.